ACS OMEGA

Open Access

http://pubs.acs.org/journal/acsodf

Article

First-Principles Study of the Dispersion Effects in the Structures and Keto−Enol Tautomerization of Curcumin

Roichatul Madinah, Febdian Rusydi,* Rizka N. Fadilla, Vera Khoirunisa, Lusia S. P. Boli, Adhitya G. Saputro, Nur H. Hassan,* and Azizan Ahmad

Cite This: *ACS Omega* 2023, 8, 34022−34033

Read Online

ACCESS | Metrics & More | Article Recommendations | Supporting Information

ABSTRACT: Noncovalent interactions, such as dispersion, play a significant role in the stability of flexible molecules, such as curcumin. This study revealed the importance of dispersion correction in the structure and keto−enol tautomerization of curcumin, which has rarely been addressed in computational studies. We rigorously constructed all possible unique curcumin conformers in the enol and keto forms within the first-principles framework. Regardless of the different environments, we carefully explained the agreement between the computational geometry (in the gas phase) and the experimental measurement (in the polymorph) by using dispersion correction. The calculation results for the aqueous solution of conformational abundance, thermochemistry, and reaction kinetics support the experimental observations after considering the dispersion correction. The study also suggests a water-catalyzed mechanism for keto−enol tautomerization, where dispersion correction plays a role in decreasing the energy barrier and making the keto form thermochemically and kinetically favorable. Our results could be helpful in future computational studies to find a method for increasing the aqueous solubility of curcumin; hence, the potential of curcumin as a multifunctional medicine can be fully achieved.

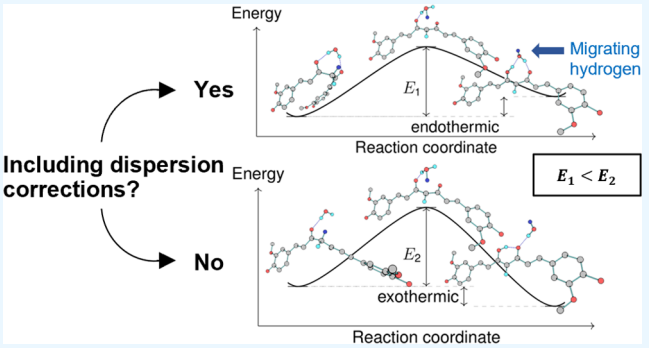

INTRODUCTION

Recent studies of curcumin have focused on its aqueous solubility and bioavailability. These two problems limit their potential therapeutic applications such as anti-inflammatory, antioxidant, and antiparasitic effects. Urošević et al.[1] and Kotha and Luthria[2] comprehensively and intensively reviewed these problems. Another extensive review by Sanphui and Bolla[3] concluded that systematic research is needed to determine the full potential of curcumin.

The study of curcumin structures can address its aqueous solubility and bioavailability problems. It is well known that stereochemical features influence the chemical properties of a molecule, as shown by curcumin. Curcumin exists in solid form as a keto−enol tautomer (see Figure 1).[4,5] The keto form is dominant in neutral aqueous solution[6−8] and in acidic aqueous solution.[9,10] In contrast, the enol form is dominant in basic aqueous solutions.[10]

Despite the urgent need to solve the problems of aqueous solubility and bioavailability, relatively few studies have focused on the structure of curcumin. The first experimental report on the structure of curcumin was published by Tønnesen et al.[11] in 1982, followed by Ishigami et al.[12] in 1999. The 17-year interval shows the slow progress of curcumin structure research, as noted by Sanphui and Bolla[3] in their review. They identified six unique conformers of curcumin, whereas

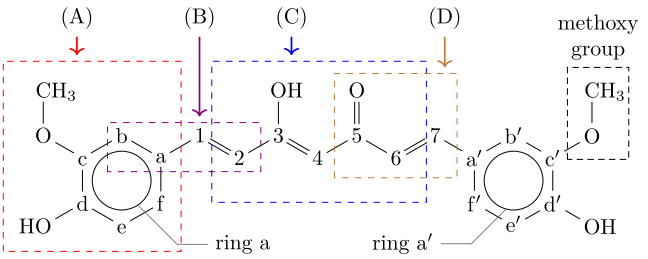

Figure 1. Skeleton structure of enol curcumin. Atoms 1−7 and a−f (without and with the prime) refer to carbon atoms. The keto form has a similar structure; however, the H atom bonded to the O^3 atom (the oxygen bonded to the carbon at 3) is displaced to the carbon at 4. Boxes (A−D) are model compounds truncated from curcumin to determine the significant torsion angle in this study (Conformers Construction Method section).

Received: July 8, 2023
Accepted: August 18, 2023
Published: September 1, 2023

https://doi.org/10.1021/acsomega.3c04907
ACS Omega 2023, 8, 34022−34033

Slabber et al.[13] and Chatterjee et al.[14] independently identified eight.

We focused on 18 reports that discussed the curcumin structure using computational methods. Of these, 16[8,14−27] were based on quantum mechanical calculations (first-principles studies) and the other two[13,28] were based on semiempirical and molecular mechanical calculations. Although flexible molecules such as curcumin are greatly impacted by noncovalent interactions,[29,30] none of the reports discussed the effect of dispersion on its structure, yet keto−enol tautomerization. Meanwhile, it is well known that dispersion is a major contributor to noncovalent interactions. To confirm the importance of dispersion interactions in curcumin structures, we evaluated the thermochemistry and kinetics of keto−enol tautomerization in neutral aqueous solution at room temperature.

This paper reports the importance of dispersion effects in the study of curcumin structures and their keto−enol tautomerization within a rigorous first-principles framework. The report begins with a procedure for constructing possible unique stable conformers by using density functional calculations. The results and discussion are divided into topics of conformational stability, structure, abundance, and keto−enol tautomerization. The role of dispersion correction is presented for each discussion topic.

METHODS

Conformers Construction Method. As a flexible molecule, a single isolated curcumin molecule ($C_{21}H_{20}O_6$) has many possible conformers. These conformers arise from the torsion of the seven carbon linkers between the two terminal phenyl rings (Figure 1) and the torsion angles of the phenyl rings, methyl groups, and hydroxy groups. In addition to conformers, curcumin can also exist in enol and keto forms. The following illustrates a large number of possible curcumin conformers in the enol form: If only 10 torsion angles from one methyl to another methyl group via the carbon linkers were taken into consideration, with each torsion angle having four basic conformations (*cis*, *gauche*, *anticlinal*, and *trans*),[31] there would be 4×10^4 possible conformers.

Instead of using the existing conformers from the aforementioned studies,[3,8,13−28] we constructed curcumin conformers using a first-principles framework. We laid the construction based on the enol form, while the whole keto form was derived from the enol form, preventing missing possible conformers in the keto form due to its symmetry (Figure 1). We reduced the number of possible conformers in the enol form because not all were unique after reaching their optimized geometry. It was achieved by finding the most stable conformers of the model compounds based on the four parts of curcumin, as shown in Figure 1. The geometry optimization of the conformers was carried out using density functional calculations with APFD/6-311++G(d,p). The model compounds were (A) guaiacol, $C_7H_8O_2$; (B) 1,3-butadiene, C_4H_6; (C) acetylacetone, $C_5H_8O_2$; and (D) acrolein, C_3H_4O.

Table 1 presents the results of the procedure using a first-principles framework. Each model compound was combined to form curcumin. The number of possible unique conformers is now the product of all possible conformations [numbers in column (4)], which was 16. The keto form was constructed from each of the 16 conformers by relocating H from the O^3 to carbon at 4 (Figure 1). Owing to its symmetry, the keto form has only 10 possible unique conformers.

Table 1. Most Stable Conformation from Model Compounds (A), (B), (C), and (D) of Figure 1[a,b,c]

(1)	(2)	(3)	(4)	(1)	(2)	(3)	(4)
θ_1	H−O−d−c	c	1	θ_6	O−5−4−3	c	1
θ_2	C−O−c−d	t	1	θ_7	O−5−6−7	t, c	2
θ_3	b−a−1−2	t, g	2	θ_8	6−7−a′−b′	t, g	2
θ_4	1−2−3−4	t, g	2	θ_9	H−O−d′−c′	c	1
θ_5	H−O−3−4	c	1	θ_{10}	C−O−c′−d′	t	1

[a]Column 1 and 2: the torsion angle and its definition. [b]Column 3: the most stable conformation after geometry optimization, with *c* for *cis*, *g* for *gauche*, and *t* for *trans*. [c]Column 4: the total conformation for the respective θ.

The results in Table 1 show that the torsion angles θ_3, θ_4, θ_7, and θ_8 distinguish one possible unique conformer from the other. The remaining torsion angle had only one conformation, as shown in Table 1: column 3. Therefore, we named the conformers (θ_3, θ_4, θ_7, θ_8). For instance, the structure in Figure 1 is ctcc conformer, where (θ_3 = *cis*, θ_4 = *trans*, θ_7 = *cis*, and θ_8 = *cis*).

The torsion angles (θ_3, θ_8) dictated the orientation of the methoxy groups with respect to those of 3−O (for ring a) and 5−O (for ring a′). Using the Newman projection orientation, the methoxy group may have two possible orientations: *syn* or *anti*. Therefore, the methoxy groups in conformer ctcc (Figure 1) have *syn* (ring a) and *syn* (ring a′) or *syn*−*syn* orientations.

Computational Method. *Thermochemical and Kinetics Quantities.* In this study, the reaction energy and energy barrier represent the thermochemistry and kinetics of keto−enol tautomerization. Calculations of these two energies require a potential pathway for tautomerization. Construction of the tautomerization pathway requires three computational quantities: (1) conformational structures, (2) stability order, and (3) conformational abundance of all possible unique conformers in both the keto and enol forms. The conformational structures along the pathway provide the mechanism for keto−enol tautomerization.

Computational Routines. The routines for developing a potential pathway of tautomerization are as follows. Routine 1 was to find the optimized geometry for all possible unique conformers with thermal correction at room temperature in the ground state (the stable structure). The results were all three computational quantities required in the gas phase (i.e., a single isolated curcumin), with additional calculations using the Boltzmann distribution for the conformational abundance. Routine 2 was to calculate all three required computational quantities when curcumin was in neutral aqueous solution. The conformational abundance from Routine 2 was used to select the representative curcumin conformer for constructing the potential tautomerization pathway and mechanism. Routine 3 was to find the correct structure in the transition state of the tautomerization of the representative curcumins conformer.

All routines were performed on the basis of density functional theory (DFT),[32,33] integrated into the Gaussian 16 software.[34] The self-consistent field (SCF) routine, which was the core routine in the DFT calculations, had an energy threshold of 10^{-6} eV. Routine 1 was the standard for any first-principles calculation. Routine 2 used two approaches: a polarizable continuum model (PCM, Routine 2a) and a PCM coupled with one H_2O (Routine 2b). Routine 3 used three combined methods: following the vibrational mode that led to the transition state described by Rusydi et al.,[35] transition state

https://doi.org/10.1021/acsomega.3c04907
ACS Omega 2023, 8, 34022−34033

optimization, and intrinsic reaction coordinate (IRC) calculations to ensure that the transition state connected the desired initial and final states, which were the selected conformers of keto and enol forms from Routine 2.

Dispersion Effect Study through DFT Calculations. The dispersion effects were studied by performing all routines using five different exchange-correlation functionals (XCs) but with one basis set, 6-311++G(d,p). These XCs are listed in Table 2.

Table 2. Code of the Exchange-Correlation Functionals Used Throughout This Manuscript

code	name
(1)	APFD
(2)	M06-2X
(3)	B3LYP
(4)	B3LYP with the GD3 empirical dispersion correction
(5)	CAM-B3LYP

B3LYP does not consider dispersion correction;[36] therefore, it was used as a reference for studying the dispersion effects obtained by other XCs. B3LYP with GD3 and APFD differs in the empirical dispersion add-on. B3LYP with GD3 expresses the dispersion interaction by a multiple expansion,[37] while APFD expresses it by a spherical atom model.[38] On the other hand, M06-2X handles the dispersion correction by parametrizing the exchange part.[39] CAM-B3LYP only corrects long-range covalent interactions, which is commonly important for the polarizability of long chains,[40] such as curcumin. However, APFD was the primary XC throughout this study to complement the previous 12 computational studies[14−23,25,26] that used B3LYP, whereas others used the Hartree−Fock method,[6] plane-wave PBE,[24] and M06-2X.[8,27] It is worth mentioning that we did not consider vdW density functionals, which include dispersion correction computed from electron density. Despite the high accuracy, these functionals are commonly used for metallic systems[41,42] with a high computational cost.[43]

RESULTS AND DISCUSSION

Conformational Stability. *Stability Order.* Routine 1 identified 16 unique ground-state conformers in the enol form and 10 in the keto form with varying stabilities (their Cartesian coordinates are listed in Tables S5−S30). Figure 2 shows the order of stability of these conformers with the group of order based on their electronic energy levels for APFD, M06-2X, and B3LYP XCs (the other two XCs are presented in Figure S1). The energy span between the most and least stable conformers was approx. 0.25 eV (5.8 kcal/mol). Table 3 shows the group of order according to the relative electronic energy. In addition to the conformational stability results, we noted that APFD completed Routine 1 faster than M06-2X and B3LYP did, as shown in Table S1.

Table 3. Group of Stability Order from Figure 2 Based on Relative Electronic Energy ($E_{rel.}$)[a]

		conformation			
group of order	$E_{rel.}$ (eV)	θ_3	θ_4	θ_7	θ_8
I	∼0.00	α	t	c	β
II	∼0.07	α	t	t	t
III	∼0.10	α	γ	γ	β
IV	∼0.14	c	c	c	β
V	>0.17	α	c	t	β

[a]The last four columns list the conformation similarity among the group with α, β, and γ may take the conformation of cis or trans and $\alpha \neq \beta \neq \gamma$.

Conformational Planarity. The seven carbon linkers in the enol form tended to be planar but not in the keto form. Figure 3 shows that the most stable conformers (e1 and k1) were obtained by using APFD. Conformational planarity can be quantitatively assigned to torsion angles of 2−3−4−5 or θ_{11}. Table 4 shows the θ_{11} values for all conformers in both forms. For the enol form, the θ_{11} value was approx. 180° (*trans*). For the keto form, it was approx. 63−77° (*gauche*). These planarity results are consistent with those of the aforementioned computational studies.[8,14,18,20−22,25,26]

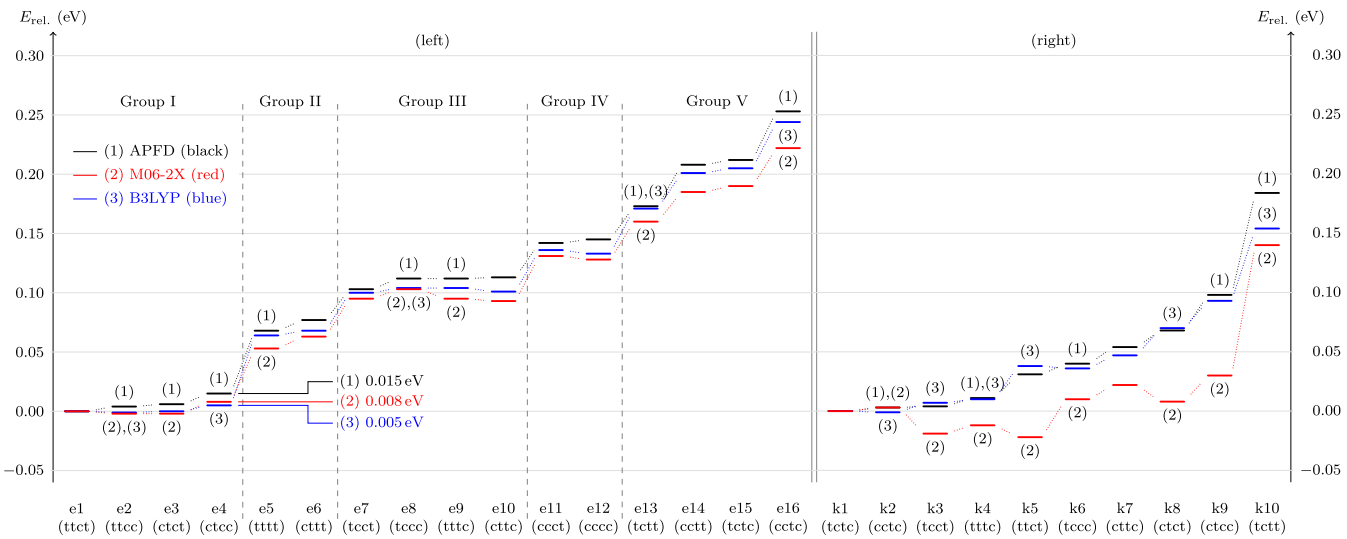

Figure 2. Conformational stability order of the enol (left) and keto (right) forms, according to their relative electronic energy ($E_{rel.}$). The reference energies for the enol and keto forms were the energy of e1 (ttct) and that of k1 (tctc), respectively.

https://doi.org/10.1021/acsomega.3c04907
ACS Omega 2023, 8, 34022−34033

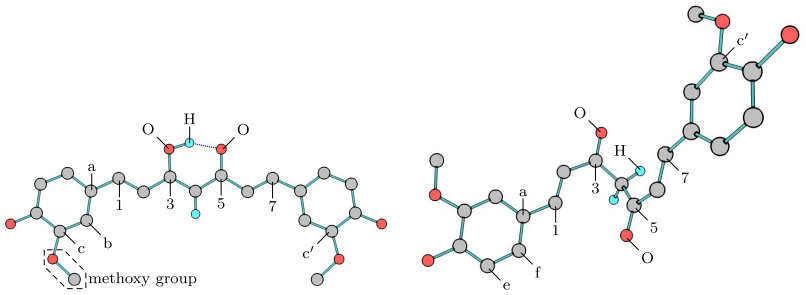

(a) Enol, ttct (e1) (b) Keto, tctc (k1)

Figure 3. Visualization of the most stable single isolated conformers using APFD. Atom numbering is shown in Figure 1. While the enol form tends to be planar, the keto form is bent at atom 4. The other conformers resemble the planarity of these two conformers, as shown in Figure S2. The geometrical parameters of these two conformers are given in Table S2.

Table 4. Value of θ_{11} Obtained by APFD

conformer		θ_{11}	conformer		θ_{11}	conformer		θ_{11}
e1	ttct	180.0°	e9	tttc	180.0°	k1	tctc	72.6°
e2	ttcc	180.0°	e10	cttc	180.0°	k2	cctc	72.3°
e3	ctct	180.0°	e11	ccct	179.6°	k3	tcct	76.6°
e4	ctcc	180.0°	e12	cccc	179.8°	k4	tttc	63.0°
e5	tttt	180.0°	e13	tctt	179.6°	k5	ttct	69.0°
e6	ctct	180.0°	e14	cctt	179.5°	k6	tccc	75.7°
e7	tcct	180.0°	e15	tctc	179.6°	k7	cttc	64.5°
e8	tccc	180.0°	e16	cctc	179.3°	k8	ctct	73.1°
						k9	ctcc	69.7°
						k10	tctt	72.5°

Characterization by Four Torsion Angles. Owing to their planarity, the stability of the enol form can be characterized by torsion angles (θ_4, θ_7) followed by (θ_3, θ_8). The combination of (θ_4, θ_7) = (t, c) resulted in the most stable structures in which the distance between the two phenyl rings was the longest. The opposite combination, (θ_4, θ_7) = (c, t), resulted in the least stable compounds, in which the distance between the two phenyl rings was the shortest. The combination of (θ_4, θ_7) classes the 16 conformers into five groups, as shown in Table 3.

The stability of conformers with the same (θ_4, θ_7) was then determined using a combination of (θ_3, θ_8). The most stable conformers were always (t, t), and the least stable conformers were always (c, c). Meanwhile, the combination of (t, c) or (c, t) was in the middle.

In contrast, the stability of the keto form was not determined by the torsion angles (θ_3, θ_4, θ_7, and θ_8) alone. The bending of the seven carbon linkers, defined by θ_{11}, complicated the characterization using the torsion angles as in the enol form. The orientation (θ_3, θ_8) = (c, c) does not always correspond to the *syn*−*syn* orientation, and (θ_3, θ_8) = (t, t) is not always the *anti*−*anti* orientation, as is always the case in the enol form. However, the torsion angles (θ_3, θ_4, θ_7, and θ_8) are still unique to the structure of the keto form.

Conformational Name. For consistency, the conformers in this report were named using the torsion angles (θ_3, θ_4, θ_7, and θ_8), as it had been used in Figures 2 and 3 and Table 4. This naming method differs from the method used by Sanphui and Bolla,[3] who named the conformers based on the orientation of the methoxy groups relative to 3−O and 5−O of Figure 1.

Dispersion Effects on the Stability Order. As discussed in the Characterization by Four Torsion Angles section, torsion angles (θ_3, θ_8) affected the stability within a given group. For example, in Group I of Figure 2, the B3LYP results showed that the (θ_3, θ_8) = (c, c) orientation destabilized conformer e4 (ctcc) by 0.005 eV. In contrast, the APFD and M06-2X results show that the same conformer was destabilized by 0.015 and 0.008 eV, respectively. These energy differences were considered significant since they were higher than the computational energy threshold (10^{-6} eV). This difference from the B3LYP results indicates the effect of the dispersion correction. The effect was present in all groups, where the APFD and M06-2X results differed from the B3LYP results.

Conformational Optimized Structures. *Relation with Previous Studies.* Most computational studies used conformers e1 (ttct) and e4 (ctcc), as shown in Table 5. These conformers belong to Group I in Table 3, along with conformers e2 (ttcc) and e3 (ctct). In a first-principles framework, all conformers in this group are highly predictable. It is conceivable that most computational studies on the enol form of curcumin have used an e1-like structure, owing to its symmetry, simplifying computational problems. In the case of the keto form (Table 6), conformer k9 (ctcc) was the most computationally studied structure because conformer k9 was derived from conformer e4. Furthermore, both tables show that four of the five computational studies that investigated conformer k9 also studied conformer e4.

Conformers e3 (ctct), e4 (ctcc), e5 (tttt), and e7 (tcct) were experimentally observed. Of these, conformers e4 and e5 were the most favorable structures in the experiment. The former can be found in the form of a solute and polymorph, whereas the latter is found only in the form of a polymorph. In the form of a polymorph, the measured geometries were used to verify the calculated optimized structures of a single isolated curcumin. Overall, all XCs obtained structures of conformers e4, e5, and e7, which are comparable to the measured values, as shown in Table S3. Most parameter values were within the B3LYP mean unsigned error (MUE): 0.017 Å and 1.4° for the bond length and angle, respectively.[48]

Large Discrepancies in Geometry. Although most of the calculated parameters agree with the experimental measurement, some discrepancies exceed the aforementioned MUE. Table 7 lists the parameters with large discrepancies. The parameters in parentheses had strikingly large discrepancies; they were all located in the peripheral and enolic regions. These discrepancies can be explained when the dispersion interaction was considered, as discussed in the following paragraphs.

https://doi.org/10.1021/acsomega.3c04907
ACS Omega 2023, 8, 34022−34033

Table 5. Compilation of Conformational Structures Study for the Enol Form[a]

(1) this work		(2) other works	
conformer		(a) computational	(b) experimental
e1	ttct	(i)[8,14,18,20,22,25]	(0)[8,14,18,25−27]
		(ii) in DMSO[13]	
		(ii) in ethanol[26]	
		(ii) in water[17,27]	
e2	ttcc	(i)[14,18,23]	(0)[14,18]
e3	ctct	(i)[14,22]	(0)[14]
			(iii)[44]
e4	ctcc	(i)[14,15,18,20,25,28]	(0)[6,14,18]
		(ii) in DMSO[13]	(ii) in DCM[45]
		(ii) in acetonitrile[19,21]	(iv) form 2[5,24]
		(ii) in MeOH[22]	(iv)[4]
		(ii) dimer in water[6]	
e5	tttt	(i)[14]	(0)[14]
			(iv) form 1[5,24]
			(iv)[12,46,47]
e6	cttt	(i)[14,18]	(0)[14,18]
e7	tcct	(i)[14]	(0)[14]
			(iv) form 1[11]
e8	tccc	n.r.	n.r.
e9	tttc	(i)[14,18]	(0)[14,18]
e10	cttc	(i)[18]	(0)[18]
e11	ccct	n.r.	n.r.
e12	cccc	n.r.	n.r.
e13	tctt	(i)[18]	(0)[18]
e14	cctt	(i)[18]	(0)[18]
e15	tctc	n.r.	n.r.
e16	cctc	(i)[18]	(0)[18]

[a]Other works (column 2) studied curcumin in the (i) gas phase, (ii) solution, (iii) cocrystal, and (iv) polymorph/crystal. The (0) is for some experimental works that did not measure the geometry, but reported it from their computational study.

Table 6. Continuation of Table 5 for the Keto Form[a]

(1) this work		(2) other works	
conformer		(a) computational	(b) experimental
k1	tctc	n.r.	n.r.
k2	cctc	(i)[25]	n.r.
k3	tcct	n.r.	n.r.
k4	tttc	n.r.	n.r.
k5	ttct	(i)[8,20]	n.r.
		(ii) in water[27]	
k6	tccc	n.r.	n.r.
k7	cttc	(i)[25]	n.r.
k8	ctct	(i)[23]	n.r.
		(ii) in water[17]	
k9	ctcc	(i)[15,16,18]	n.r.
		(ii) in acetonitrile[21]	
		(ii) in MeOH[22]	
k10	tctt	n.r.	n.r.

[a]Check the note in Table 5.

Although intermolecular interactions exist only in curcumin polymorphs, intramolecular interactions still exist in isolated curcumin. Parameters numbers 12−14 were intramolecular hydrogen bonds experimentally discussed by Parimita et al.[46] These noncovalent interactions, inter- and intramolecularly, in the periphery and enolic regions rotate θ_{11}, leading to discrepancies between the calculated and experimental geometric parameters exceeding the tolerance level.

Intramolecular interactions are relevant for studying a single isolated curcumin (in the gas phase). Our results show that dispersion correction affected the ground-state optimized structure (for the stability in Figure 2 and for the geometry in Figure S2). Since dispersion interaction is a part of intramolecularly noncovalent interactions, the results strongly suggest that dispersion interaction must be considered when studying curcumin, even in the gas phase.

Curcumin in the Aqueous Solution at Room Temperature. *Effects on the Stability Order.* All of the XCs found that the thermal correction at room temperature was not equal for all conformers, with some being more affected than others (see Figure S3). We examined the APFD results in detail, as shown in Figure 4. The effect was particularly noticeable for conformers e4 (ctcc), e12 (cccc), and k8 (ctct) in aqueous solution. Conformer e4 was destabilized in the aqueous solution by about 1.7 kcal/mol, while conformers e12 and k8 were stabilized by 2.7 and 2.8 kcal/mol, respectively.

Effects on the Conformational Abundance. The conformational abundance reflects the thermal correction, as shown in Figure 5. The relative abundance of conformer e4 decreased from 22.3% in the gas phase to 1.0% in aqueous solution. In contrast, the abundance of conformers e12 and k8 increased from 0.4 and 11.0% in the gas phase to 22.3 and 78.3%, respectively, in the aqueous solution.

Dispersion Effects. Using the B3LYP results as a reference, the dispersion effects were observed in the conformational abundance results. Dispersion correction changed the relative abundance significantly in some conformers, namely, e4, e12, k3, k5, k8, and k10, where the difference was higher than 10% (see Table S4 for the difference from all conformers). This correction caused the favorable conformers in the aqueous solution to shift from conformer e12 (30% by B3LYP) to conformer k8 (80% by APFD). Furthermore, the correction results by APFD were mostly in contrast to those of M06-2X. It is possible that the difference in handling dispersion correction caused these two XCs to yield unequal effects in aqueous solution at room temperature.

Keto−Enol Tautomerization Mechanism. *Selection of Conformers.* Conformer k8 (ctct) represented the keto−enol tautomerization study in its initial state. It was the most abundant conformer in the APFD results. The IRC calculations from Routine 3 suggest that the final state was conformer e3 (ctct), which was coincidentally the origin of conformer k8.

Tautomerization Pathway. Overall, all XCs obtained a one-step potential pathway for keto−enol tautomerization. Table 8 summarizes the results. All XCs agreed with the tendency of the reaction energy (thermochemistry) and energy barrier (kinetic). Thermochemically, the tautomerization shifted toward endergonicity when the environment changed from the gas phase (column a) to the aqueous solution (columns b and c). Kinetically, a change in the environment decreased the energy barrier.

The detailed mechanism and dispersion correction role are discussed in the following paragraphs. These discussions are based on the conformational structures in the initial, transition, and final states, as shown in Figure 6 and Table 9.

Water-Catalyzed Mechanism. The X-type structures in Figure 6 were obtained for tautomerization in the gas phase and aqueous solution. Without explicit H_2O, the mechanism

https://doi.org/10.1021/acsomega.3c04907
ACS Omega 2023, 8, 34022−34033

Table 7. Geometrical Parameter Discrepancy of Conformers e4, e5, and e7 between the APFD and Experimental Results[a,b,c,d]

no.	parameter	e4[5]	e4[4]	e5[12]	e5[46]	e7[11]
	(a) the carbon linker, *R* in Å and *A* in deg.					
2.	R: 4−5	w.t	w.t	+0.034	n.r.	+0.028
3.	R: 6−7	n.r.	w.t	+0.022	n.r.	w.t
(4)	R: 7−a′	n.r.	n.r.	−0.023	n.r.	w.t
5.	A: a−1−2	n.r.	n.r.	−1.6	n.r.	+2.8
6.	A: 4−5−6	n.r.	n.r.	−2.3	n.r.	−3.8
	(b) the enolic region, *R* in Å and *A* in deg.					
7.	R: 3−O	w.t	w.t	+0.023	n.r.	w.t
8.	R: 5−O	w.t	−0.019	−0.030	n.r.	−0.054
(9)	R: O^3−H	+0.076	w.t	−0.148	−0.248	n.r.
10.	A: O−3−2	n.r.	−2.7	n.r.	n.r.	n.r.
(11)	A: O −5−6	n.r.	+4.2	n.r.	n.r.	n.r.
(12)	R: H^3···O^5	n.r.	+0.017	+0.198	+0.278	n.r.
(13)	R: O^3···O^5	n.r.	w.t	+0.040	+0.039	n.r.
(14)	A: O^3···H···O^5	n.r.	−6.6	−1.6	w.t	n.r.
	(c) the phenyl ring, *R* in Å and *A* in deg.					
15.	R: d−O	n.r.	n.r.	−0.022	n.r.	−0.024
16.	R: O−$C^{c'}$	n.r.	n.r.	−0.024	n.r.	−0.027
(17)	R: O···H^d	n.r.	n.r.	n.r.	+0.116	n.r.
(18)	R: O···$H^{d'}$	n.r.	n.r.	n.r.	+0.196	n.r.
19.	R: H^d···O^c	n.r.	n.r.	n.r.	−0.070	n.r.
20.	R: $H^{d'}$···$O^{c'}$	n.r.	n.r.	n.r.	−0.261	n.r.
21.	R: O^d···O^c	n.r.	n.r.	n.r.	−0.047	n.r.
22.	R: $O^{d'}$···$O^{c'}$	n.r.	n.r.	n.r.	−0.073	n.r.
(23)	A: H···O^d···O^c	n.r.	n.r.	n.r.	−6.1	n.r.
(24)	A: H···$O^{d'}$···$O^{c'}$	n.r.	n.r.	n.r.	+3.9	n.r.
	(d) the torsion angle, all in deg.					
(25)	C−O−c−d (θ_2)	n.r.	n.r.	+6.8	n.r.	n.r.
(26)	b−c−O−C	n.r.	n.r.	−5.0	n.r.	−3.9
27.	O−c′−d′−O	n.r.	−3.4	n.r.	n.r.	n.r.
(28)	b−a−1−2	n.r.	n.r.	−4.2	n.r.	−22.9
29.	a−1−2−3	n.r.	+1.7	n.r.	n.r.	n.r.
(30)	1−2−3−4 (θ_4)	n.r.	n.r.	+3.1	n.r.	−12.3
31.	O−5−4− 3 (θ_6)	n.r.	n.r.	−2.3	n.r.	n.r.
(32)	O−5−6− 7 (θ_7)	n.r.	n.r.	+15.2	n.r.	−3.1
33.	4−5−6−7	n.r.	+1.5	n.r.	n.r.	n.r.
(34)	6−7− a′− f′ (θ_8)	n.r.	n.r.	+25.0	n.r.	n.r.
(35)	6−7−a′− b′	n.r.	n.r.	−25.1	n.r.	−5.7

[a]Parameter No. 1 was θ_{11} (shown in Table 4). [b]Parameter in parentheses = the periphery regions; A···B = noncovalent bond between A and B. [c]Notations such as "C^{c}" = C atom that bound to the atom at c. [d]"n.r." = no report; "w.t." = within the tolerance (0.017 Å or 1.4°).

resembles that of hydroxycarbene isomerization (HCOH → H_2CO)[49,50] and methylhydroxycarbene isomerization (CH_3−C−OH → CH_3−CH = O or CH_2=C−OH).[51] The energy barriers of these two isomerizations are theoretically high for small molecules (32.28 kcal/mol), yet they were experimentally observed with a short half-life (2 h). The short half-life suggested that the isomerizations underwent quantum tunneling. The same mechanism may be possible for keto−enol tautomerization in the gas phase. Since the probability of quantum tunneling was only proportional to the square root of the barrier height [$T \propto \exp(-\sqrt{E_b})$],[52] it can explain the quantum tunneling possibility occurring in the high energy barrier of keto−enol tautomerization as shown in Table 8. The quantum tunneling mechanism is possible for the tautomerization of heavy molecules as suggested by Schleif et al.[53,54]

Modeling an aqueous solution solely with a PCM (Routine 2a) cannot decrease the energy barrier. It was demonstrated by Fadilla et al.[55] and Susanti et al.[56] that the energy barrier failed to decrease for the hydroxycarbene and methylhydroxycarbene isomerizations, respectively. It was also the case in this study. The results align with the work of Chatterjee et al.,[14] who studied the keto−enol tautomerization of curcumin in a methanol solution modeled solely by PCM. They reported an energy barrier of 50.51 kcal/mol, which was the same order as that of the aqueous solution in this work.

The results from PCM coupled with one H_2O calculation (Routine 2b) suggest a water-catalyzed mechanism. The mechanism was visualized in Y- and Z-type structures. H_2O formed a complex with curcumin in the initial state and rotated θ_{11} toward 90° (*anticlinal*). The *anticlinal* orientation of θ_{11} directed one of the H atoms at 4 in conformer k8 toward H_2O. This direction assists the hydrogen migration toward H_2O to achieve the transition state. The same mechanism is suggested by Jin et al.[57] for the case of keto−enol tautomerization of acyloxy methyl ketone.

Role of H_2O in the Transition State. Our results suggest that H_2O plays a crucial role in the transition state. In this state, θ_{11} was in an *anticlinal* orientation following its initial

https://doi.org/10.1021/acsomega.3c04907
ACS Omega 2023, 8, 34022−34033

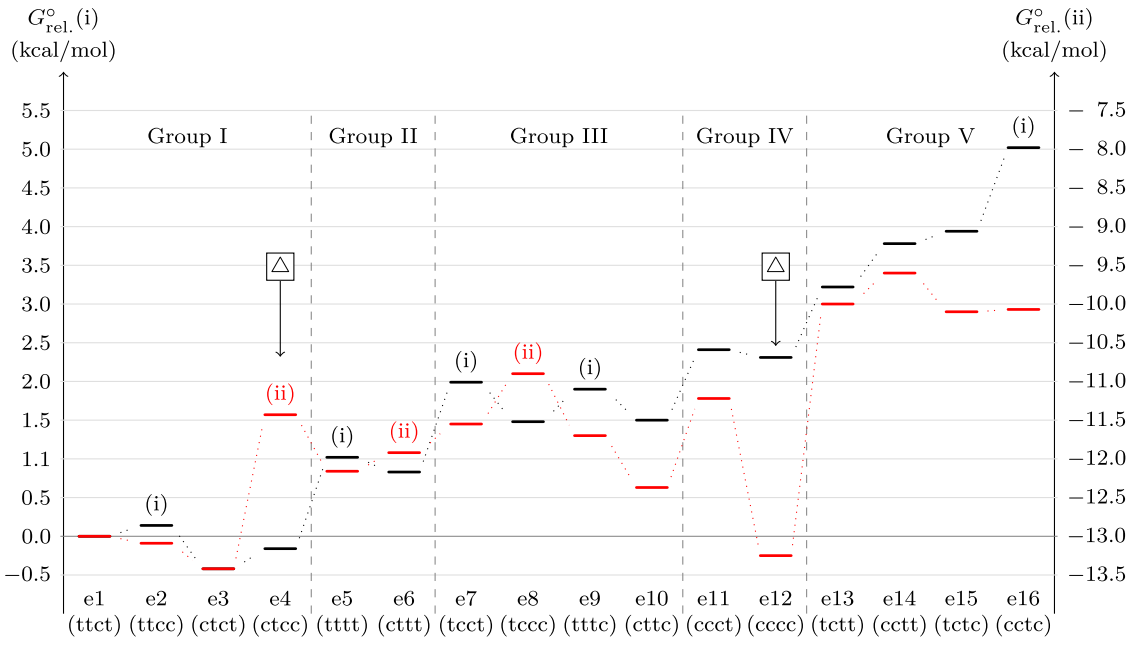

(a) The enol form

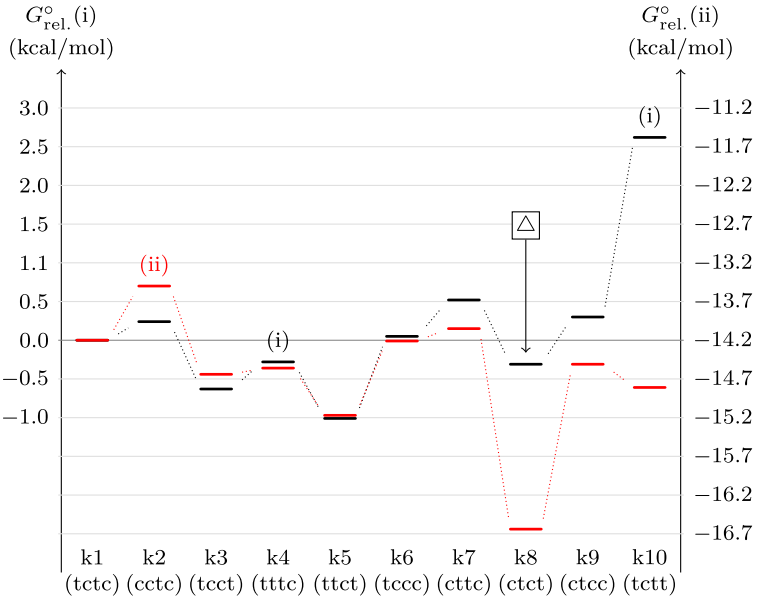

(b) The keto form

Figure 4. Conformational stability order obtained by APFD with thermal correction at room temperature in (i) the gas phase and (ii) the aqueous solution. The energy is calculated in relative standard Gibbs free energy ($G^{\circ}_{rel.}$). Conformers with sign △ were the most affected by the thermal correction in the aqueous solution.

state. This orientation allowed H_2O to take the migrating H and donate its own H to the O^3 of curcumin. The 3−O bond length was shortened, as listed in Table 9 (parameter No. 7). It implies that the structures in the transition state were stabilized in the presence of H_2O. Eventually, in the final state, the H at O^3 was not from curcumin but from H_2O instead. The net result of these processes was that the energy barrier decreased by approx. 18 to 24 kcal/mol (32 to 44% decreasing).

The role of H_2O in the keto−enol tautomerization of curcumin resembles that of acetone, $CH_3{-}C(=O){-}CH_3 \rightarrow CH_2{=}C(-OH){-}CH_3$. Cucinotta et al.[58] used the first-principles molecular dynamics method and concluded that the H_2O catalyzed the tautomerization by taking and donating hydrogen from and to the acetone precisely like in this study. They calculated that one H_2O decreased the barrier by approx. 12 kcal/mol, and 28 H_2O molecules decreased it by up to 20 kcal/mol (20 to 33% decreasing), which is the same order as the keto−enol tautomerization of curcumin.

Dispersion Effects on the Tautomerization Energy. The water-catalyzed mechanism can be used to evaluate the importance of dispersion correction. Without dispersion correction, the role of H_2O can be studied using B3LYP.

https://doi.org/10.1021/acsomega.3c04907
ACS Omega 2023, 8, 34022−34033

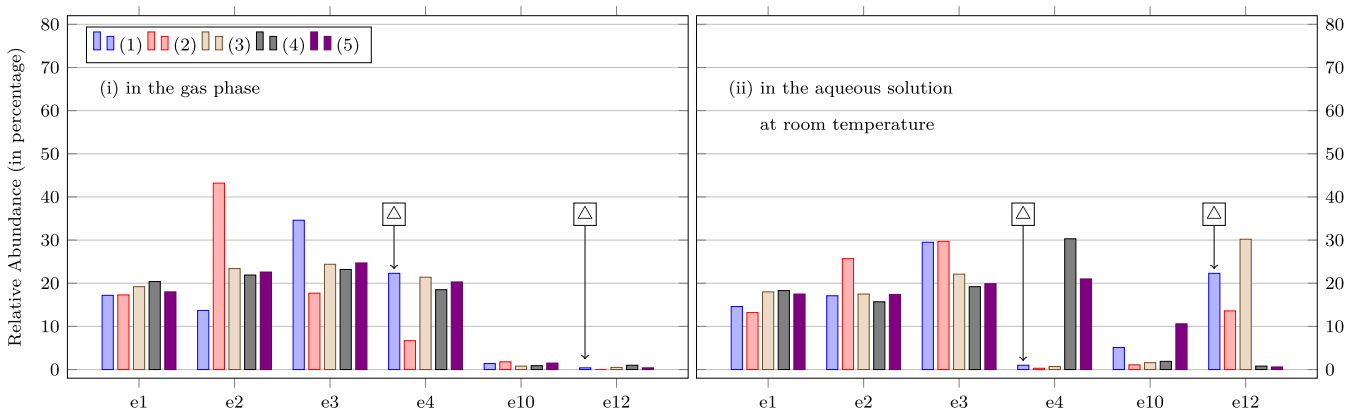

(a) The enol form.

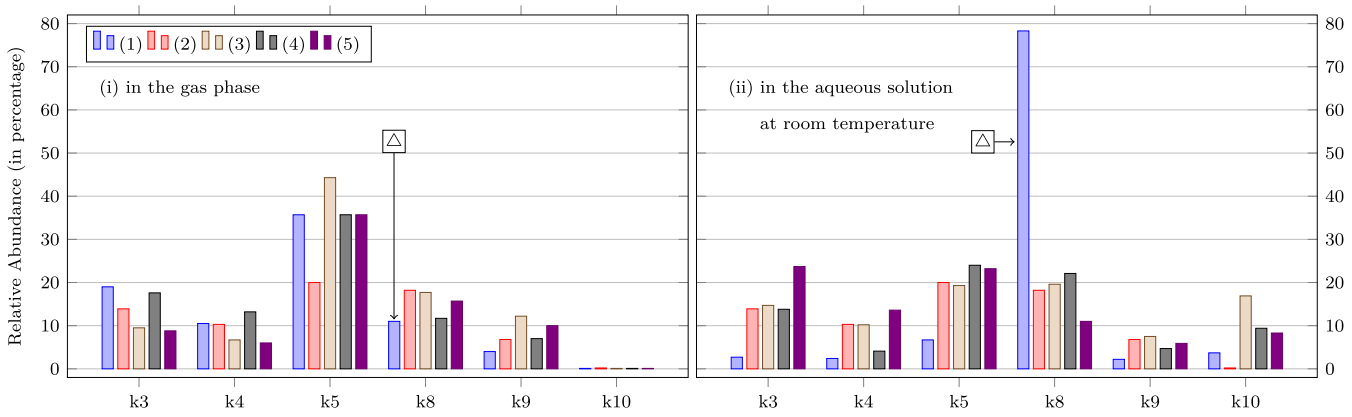

(b) The keto form.

Figure 5. Relative abundance exceeded 10% of that of each form. The XCs legend refers to Table 2: (1) APFD, (2) M06-2X, (3) B3LYP, (4) B3LYP with GD3, and (5) CAM-B3LYP. The sign △ refers to the three conformers shown in Figure 4. The complete plot for all conformers is provided in Figure S4.

Table 8. Reaction Energy and the Energy Barrier Calculated from the One-Step Tautomerization Pathway in Terms of the Standard Gibbs Free Energy (kcal/mol)

		reaction energy, E_R			energy barrier, E_B		
XC		(a)	(b)	(c)	(a)	(b)	(c)
(1)	APFD	−5.35	−1.98	1.90	53.20	52.67	29.88
(2)	M06-2X	−3.50	−3.06	−4.06	56.08	53.48	32.11
(3)	B3LYP	−4.80	−3.31	−3.95	54.43	51.76	35.61
(4)	B3LYP with GD3	−3.60	−1.78	−2.84	55.26	52.73	34.29
(5)	CAM-B3LYP	−4.27	−2.93	−2.58	56.01	53.37	36.01

However, the correction changed the conformational structures in all three states, hence the thermochemical and kinetic energy of tautomerization. The detailed discussion of the changes is as follows.

Conformational Structures in the Aqueous Solution. A comparison of the Y- and Z-type structures shows different conformational structures with and without dispersion correction. The correction contributed three contrasts that made the Y-and Z-type distinguishable. First, two hydrogen bonds were formed between curcumin and water in the Y-type structure, whereas only one was present in the Z-type structure. Second, the new hydrogen bond distance was shorter in the Y- than in the Z-type structure (Table 9, parameter No. 36). Third, in the enol form (the final state), the H atom at O^3 prefers a noncovalent bond with water rather than with O^5. This preference was reflected by the shortening of the O^3−H covalent bond length (No. 9) and elongation of the H^3−O^5 covalent bond length (No. 12).

Effects on Thermochemistry and Kinetics. The net result of the geometric change after dispersion correction was the stabilization of the initial and final states. This stabilization could be quantified using the complex formation energy, as presented in Table 10.

Four of five XCs stabilized the structures in the initial state (column a) to a greater extent than in the final state (column b). Consequently, the energy difference (column c) was positive. These results explain the endergonic tendency of the

https://doi.org/10.1021/acsomega.3c04907
ACS Omega 2023, 8, 34022−34033

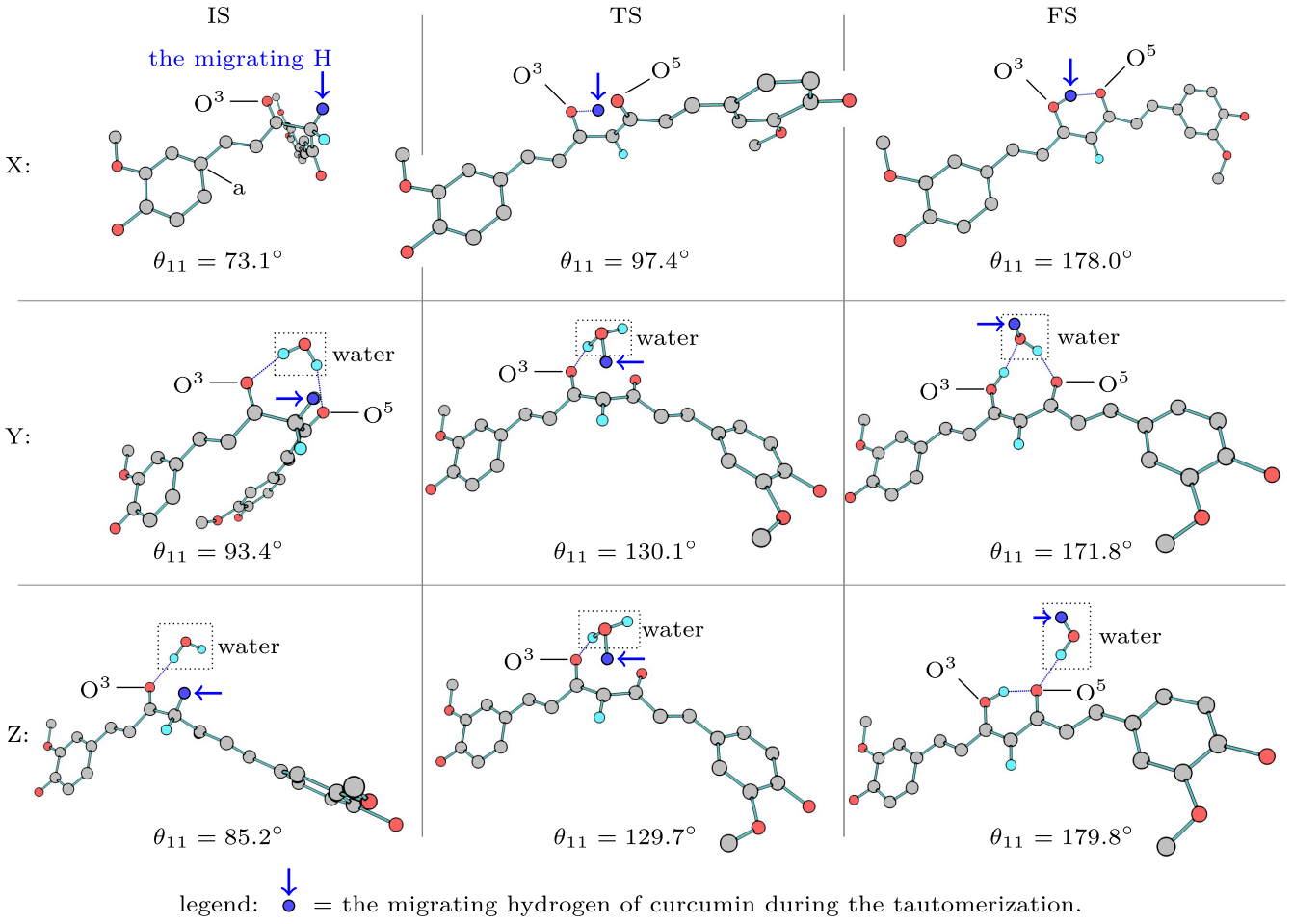

Figure 6. Visualization of conformational structures in the initial, transition, and final states of k8-e3 tautomerization. The X- and Y-type structures were related to the pathway determined by APFD via Routines 1 and 2b, respectively. The Z-type was related to the pathway determined by B3LYP via Routine 3b. All structures obtained by the B3LYP variation were Z-type structures. The ones obtained by M06-2X were Y-type for the IS and Z-type for the FS. The selected geometric parameters in the enolic region are listed in Table 9, while the Cartesian coordinates of the relevant structures in the tautomerization pathways are listed in Tables S7, S28, and S31−S37.

Table 9. Geometric Parameters (Parm.) in Enolic Region of Conformational Structures Visualized in Figure 6[a,b]

		IS			TS			FS		
no.	parm.	X	Y	Z	X	Y	Z	X	Y	Z
	(a) enolic region of curcumin, in Å									
7.	R: 3−O	1.320	1.228	1.235	1.281	1.264	1.270	1.219	1.326	1.335
(9)	R: O^3−H	n.rv.	n.rv.	n.rv.	1.247	2.374	2.389	1.016	0.991	1.004
(12)	R: $H^3\cdots O^5$	n.rv.	n.rv.	n.rv.	2.726	2.677	2.776	1.543	2.467	1.612
	(b) oxygen to the closest hydrogen of water (H_w), in Å									
36.	R: $O^3\cdots H_w$	n.rv.	1.885	1.833	n.rv.	1.433	1.442	n.rv.	n.rv.	n.rv.
37.	R: $O^5\cdots H_w$	n.rv.	1.955	4.243	n.rv.	2.481	2.676	n.rv.	1.645	1.815

[a]See note in Table 7. [b]"n.rv." = the parameter was not relevant.

keto−enol tautomerization of curcumin in an aqueous solution.

The M06-2X results were an exception, where the initial state stabilization (the keto-water complex) was less than that of the final state (the enol−water complex). The exception can be linked to its keto-water complex structure, which resembles Y-type structures rather than Z-type structures.

A similar study by Manolova et al.[8] (using M06-2X) reported similar energetic results. They reported that the enol form was more stable than the keto form after forming a complex with H_2O. The energy difference was approx. 4.0 kcal/mol. However, the addition of another H_2O to the complexes resulted in the keto-water complex being only 0.6 kcal/mol higher in energy level than the enol−water complex Their results indicate that the keto form should be dominant in the aqueous solution if there were enough H_2O in the model. Our results for APFD share the same indication, even though there was only one H_2O. Therefore, a comparison of the work of Manolova et al.[8] and our work points out the importance of dispersion correction in computational studies.

The dispersion corrections from the APFD XC yielded standout results, as shown in Table 10 (column d). The

https://doi.org/10.1021/acsomega.3c04907
ACS Omega 2023, 8, 34022−34033

Table 10. Complex Formation Energy in Terms of the Standard Gibbs Free Energy (kcal/mol) of Curcumin-Water[a,b,c,d]

		(a) k8-water		(b) e3-water		(c)	(d)	
XC		type	G°_{kw}	type	G°_{ew}	ΔG°	ΔG°_{kw}	ΔG°_{ew}
(1)	APFD	Y	−15.33	Y	−8.09	+7.24	−0.54	+5.84
(2)	M06-2X	Y	−14.81	Z	−15.37	−0.56	−0.02	−1.44
(3)	B3LYP	Z	−14.79	Z	−13.93	+0.86	0.00	0.00
(4)	B3LYP with GD3	Z	−15.29	Z	−14.53	+0.76	−0.50	−0.60
(5)	CAM-B3LYP	Z	−15.77	Z	−14.08	+1.69	−0.98	−0.15

[a]Column XC and Type: refer to Table 2 and Figure 6, respectively. [b]Column G°_{iw} = complex formation energy of $i + w \rightarrow i{-}w$, which was $G^{\circ}_{iw} = G^{\circ}_{i\text{-}w} - (G^{\circ}_{i} + G^{\circ}_{w})$. ($i$ = curcumin, the keto or enol form; w = water.) [c]Column c: $\Delta G^{\circ} = G^{\circ}_{ew} - G^{\circ}_{kw}$, which was proportional to the reaction energy in Table 8. [d]Column d: relative formation energy, ΔG°, which was the difference from the B3LYP result.

dispersion corrections obtained for each XC affected the keto and enol forms in different ways. APFD and B3LYP with the GD3 parameter greatly affected both the forms. However, only APFD predicted a positive correction for the enol form, leading to a positive reaction energy (Table 8). It implies that the dispersion correction revealed the favorability of the keto form thermochemically and kinetically, which supports experimental observations.[7,8] This analysis supports the work of Bhatia et al.,[9] who concluded that tautomerization tends toward the direction of keto formation at higher temperatures, indicating the need for a lower barrier from the enol to keto form.

CONCLUSIONS

We rigorously demonstrated the importance of dispersion correction in studying the structure and the keto−enol tautomerization of curcumin using a first-principles framework. By introducing the dispersion correction, we can relate the computationally isolated conformer structure to the experimental measurement of polymorph curcumin. Dispersion corrections changed the favorable abundance from the enol form (without correction) to the keto form (with correction). The dispersion correction consistently made the keto form favorable thermochemically and kinetically, supporting experimental observations. Furthermore, our results suggest a water-catalyzed mechanism of keto−enol tautomerization, where dispersion correction was responsible for the energy barrier decrease. Our results could be helpful in future computational studies to find a method for increasing the aqueous solubility of curcumin; hence, the potential of curcumin as a multifunctional medicine can be fully achieved.

The study also pointed out that APFD was the most suitable exchange-correlation functional for studying the structure and keto−enol tautomerization of curcumin. The dispersion correction in the APFD not only yielded standout results but also improved the accuracy of the thermochemical and kinetic quantities of keto−enol tautomerization. This improvement by APFD agrees with the work of Rayne and Forest,[59] who benchmarked various XCs (including all five XCs used in this work) against 24 isomerizations and concluded that APFD was superior to the others.

ASSOCIATED CONTENT

Supporting Information

The Supporting Information is available free of charge at https://pubs.acs.org/doi/10.1021/acsomega.3c04907.

Visualization of curcumin's stability order in the gas phase; optimized structure; thermal corrections on the stability order; relative abundance in the aqueous solution; and list of computational time, geometrical parameters discrepancy, Cartesian coordinates of the optimized structures (PDF)

AUTHOR INFORMATION

Corresponding Authors

Febdian Rusydi − *Research Center for Quantum Engineering Design, Faculty of Science and Technology and Department of Physics, Faculty of Science and Technology, Universitas Airlangga, Surabaya 60115, Indonesia;* orcid.org/0000-0002-7224-5731; Email: rusydi@fst.unair.ac.id

Nur H. Hassan − *Department of Chemical Sciences, Faculty of Science and Technology, Universiti Kebangsaan Malaysia, Bangi, Selangor 43600, Malaysia*; Email: syareeda@ukm.edu.my

Authors

Roichatul Madinah − *Department of Chemical Sciences, Faculty of Science and Technology, Universiti Kebangsaan Malaysia, Bangi, Selangor 43600, Malaysia; Research Center for Quantum Engineering Design, Faculty of Science and Technology, Universitas Airlangga, Surabaya 60115, Indonesia*

Rizka N. Fadilla − *Research Center for Quantum Engineering Design, Faculty of Science and Technology, Universitas Airlangga, Surabaya 60115, Indonesia; Department of Precision Engineering, Graduate School of Engineering, Osaka University, Osaka 565-0871, Japan*

Vera Khoirunisa − *Department of Engineering Physics, Institut Teknologi Sumatera, Lampung Selatan 35365, Indonesia; Research Center for Quantum Engineering Design, Faculty of Science and Technology, Universitas Airlangga, Surabaya 60115, Indonesia*

Lusia S. P. Boli − *Physics Study Program, Faculty of Mathematics and Natural Sciences, Universitas Jendral Soedirman, Purwokerto 53122, Indonesia; Research Center for Quantum Engineering Design, Faculty of Science and Technology, Universitas Airlangga, Surabaya 60115, Indonesia; Advanced Functional Materials Research Group, Faculty of Industrial Technology, Institut Teknologi Bandung, Bandung 40132, Indonesia;* orcid.org/0000-0002-6687-1488

Adhitya G. Saputro − *Advanced Functional Materials Research Group, Faculty of Industrial Technology, Institut Teknologi Bandung, Bandung 40132, Indonesia*

Azizan Ahmad − *Department of Chemical Sciences, Faculty of Science and Technology, Universiti Kebangsaan Malaysia, Bangi, Selangor 43600, Malaysia*

Complete contact information is available at:

https://doi.org/10.1021/acsomega.3c04907
ACS Omega 2023, 8, 34022−34033

https://pubs.acs.org/10.1021/acsomega.3c04907

Author Contributions

R.M.: formal analysis, investigation, methodology, validation, and writing—original draft. F.R.: conceptualization, methodology, writing—review and editing, and supervision. R.N.F.: formal analysis and validation. V.K.: formal analysis, validation, and writing—original draft. L.S.P.B: formal analysis and validation. A.G.S.: formal analysis. N.H.H. and A.A.: validation and supervision.

Notes

The authors declare no competing financial interest.

■ ACKNOWLEDGMENTS

This study was supported partly by Direktorat Riset dan Pengabdian Masyarakat, Deputi Bidang Penguatan Riset dan Pengembangan Kementerian Riset dan Teknologi/Badan Riset dan Inovasi Nasional, through "Penelitian Dasar Unggulan Perguruan Tinggi" (grant number 744/UN3.LPPM/PT.01.03/2023) and partly by Ministry of Higher Education Malaysia through "Fundamental Research Grant Scheme" (grant number FRGS/1/2019/STG01/UKM/02/12). All calculations using Gaussian 16 software were carried out in computational facility "Riven" at Research Center for Quantum Engineering Design, Universitas Airlangga, Indonesia. R.M. and F.R. thank Prof. Yoshitada Morikawa (Graduate School of Engineering, Osaka University, Japan) and Dr. Ira Puspitasari (Information System, Universitas Airlangga, Indonesia) for valuable discussion and support.

■ REFERENCES

(1) Urošević, M.; Nikolić, L.; Gajić, I.; Nikolić, V.; Dinić, A.; Miljković, V. Curcumin: Biological Activities and Modern Pharmaceutical Forms. *Antibiotics* **2022**, *11*, 135−162.
(2) Kotha, R. R.; Luthria, D. L. Curcumin: Biological, Pharmaceutical, Nutraceutical, and Analytical Aspects. *Molecules* **2019**, *24*, 2930−2957.
(3) Sanphui, P.; Bolla, G. Curcumin, a Biological Wonder Molecule: A Crystal Engineering Point of View. *Cryst. Growth Des.* **2018**, *18*, 5690−5711.
(4) Parameswari, A. R.; Devipriya, B.; Jenniefer, S. J.; Muthiah, P. T.; Kumaradhas, P. Low Temperature Crystal Structure of 5-Hydroxy-1,7-Bis-(4-Hydroxy-3-Methoxy-Phenyl)-Hepta-1,6-Dien-3-one. *J. Chem. Crystallogr.* **2012**, *42*, 227−231, DOI: 10.1007/s10870-011-0229-x.
(5) Sanphui, P.; Goud, N. R.; Khandavilli, U. B. R.; Bhanoth, S.; Nangia, A. New Polymorphs of Curcumin. *Chem. Commun.* **2011**, *47*, 5013−5015.
(6) Kazakova, O.; Lipkovska, N.; Barvinchenko, V. Keto-enol Tautomerism of Curcumin in the Preparation of Nanobiocomposites with Fumed Silica. *Spectrochim. Acta, Part A* **2022**, *277*, No. 121287, DOI: 10.1016/j.saa.2022.121287.
(7) Mondal, S.; Ghosh, S.; Moulik, S. P. Stability of Curcumin in Different Solvent and Solution Media: UVvisible and Steady-state Fluorescence Spectral Study. *J. Photochem. Photobiol., B* **2016**, *158*, 212−218.
(8) Manolova, Y.; Deneva, V.; Antonov, L.; Drakalska, E.; Momekova, D.; Lambov, N. The Effect of the Water on the Curcumin Tautomerism: A Quantitative Approach. *Spectrochim. Acta, Part A* **2014**, *132*, 815−820.
(9) Bhatia, N. K.; Kishor, S.; Katyal, N.; Gogoi, P.; Naranga, P.; Deep, S. Effect of pH and Temperature on Conformational Equilibria and Aggregation Behaviour of Curcumin in Aqueous Binary Mixtures of Ethanol. *RSC Adv.* **2016**, *6*, 103275−103288.
(10) Jovanovic, S. V.; Steenken, S.; Boone, C. W.; Simic, M. G. H-Atom Transfer Is A Preferred Antioxidant Mechanism of Curcumin. *J. Am. Chem. Soc.* **1999**, *121*, 9677−9681.
(11) Tønnesen, H. H.; Karlsen, J.; Mostad, A. Structural Studies of Curcuminoids. I. The Crystal Structure of Curcumin. *Acta Chem. Scand.* **1982**, *36*, 475−479, DOI: 10.3891/acta.chem.scand.36b-0475.
(12) Ishigami, Y.; Goto, M.; Masuda, T.; Takizawa, Y.; Suzuki, S. The Crystal Structure and the Fluorescent Properties of Curcumin. *J. Jpn. Soc. Colour Mater.* **1999**, *72*, 71−77.
(13) Slabber, C. A.; Grimmer, C. D.; Robinson, R. S. Solution Conformations of Curcumin in DMSO. *J. Nat. Prod.* **2016**, *79*, 2726−2730.
(14) Chatterjee, P.; Dutta, S. S.; Chakraborty, T. Tautomers and Rotamers of Curcumin: A Combined UV Spectroscopy, High-Performance Liquid Chromatography, Ion Mobility Mass Spectrometry, and Electronic Structure Theory Study. *J. Phys. Chem. A* **2022**, *126*, 1591−1604.
(15) Wright, J. S. Predicting the Antioxidant Activity of Curcumin and Curcuminoids. *J. Mol. Struct.: THEOCHEM* **2002**, *591*, 207−217.
(16) Priyadarsini, K. I.; Maity, D. K.; Naik, G. H.; Kumar, M. S.; Unnikrishnan, M. K.; Satav, J. G.; Mohan, H. Role of Phenolic O-H and Methylene Hydrogen on the Free Radical Reactons and Antioxidant Activity of Curcumin. *Free Radical Biol. Med.* **2003**, *35*, 475−484.
(17) You-Min, S.; Wang, R.-X.; Yuan, S.-L.; Lin, X.-J.; Liu, C.-B. Theoretical Study on the Antioxidant Activity of Curcumin. *Chin. J. Chem.* **2004**, *22*, 827−830, DOI: 10.1002/cjoc.20040220812.
(18) Kolev, T. M.; Velcheva, E. A.; Stamboliyska, B. A.; Spiteller, M. DFT and Experimental Studies of the Structure and Vibrational Spectra of Curcumin. *Int. J. Quantum Chem.* **2005**, *102*, 1069−1079.
(19) Shen, L.; Zhang, H.-Y.; Ji, H.-F. Successful Application of TD-DFT in Transient Absorption Spectra Assignment. *Org. Lett.* **2005**, *7*, 243−246.
(20) Balasubramanian, K. Molecular Orbital Basis for Yellow Curry Spice Curcumins Prevention of Alzheimers Disease. *J. Agric. Food Chem.* **2006**, *54*, 3512−3520.
(21) Shen, L.; Ji, H.-F. Theoretical Study on Physicochemical Properties of Curcumin. *Spectrochim. Acta, Part A* **2007**, *67*, 619−623.
(22) Benassi, R.; Ferrari, E.; Lazzari, S.; Spagnolo, F.; Saladini, M. Theoretical Study on Curcumin: A Comparison of Calculated Spectroscopic Properties with NMR, UVvis and IR Experimental Data. *J. Mol. Struct.* **2008**, *892*, 168−176.
(23) Anjomshoa, S.; Namazian, M.; Noorbala, M. R. The Effect of Solvent on Tautomerism, Acidity and Radical Stability of Curcumin and Its Derivatives Based on Thermodynamic Quantities. *J. Solution Chem.* **2016**, *45*, 1021−1030.
(24) Matlinska, M. A.; Wasylishen, R. E.; Bernard, G. M.; Terskikh, V. V.; Brinkmann, A.; Michaelis, V. K. Capturing Elusive Polymorphs of Curcumin: A Structural Characterization and Computational Study. *Cryst. Growth Des.* **2018**, *18*, 5556−5563.
(25) Nag, A.; Chakraborty, P.; Natarajan, G.; Baksi, A.; Mudedla, S. K.; Subramanian, V.; Pradeep, T. Bent Keto Form of Curcumin, Preferential Stabilization of Enol by Piperine, and Isomers of CurcuminCyclodextrin Com plexes: Insights from Ion Mobility Mass Spectrometry. *Anal. Chem.* **2018**, *90*, 8776−8784.
(26) Galasso, V.; Kova, B.; Modelli, A.; Ottaviani, M. F.; Pichierri, F. Spectroscopic and Theoretical Study of the Electronic Structure of Curcumin and Related Fragment Molecules. *J. Phys. Chem. A* **2008**, *112*, 2331−2338.
(27) Puglisi, A.; Giovannini, T.; Antonov, L.; Cappelli, C. Interplay Between Conformational and Solvent Effects in UV−visible Absorption Spectra: Curcumin Tautomers as a Case Study. *Phys. Chem. Chem. Phys.* **2019**, *21*, 15504−15514.
(28) Zsila, F.; Bikádi, Z.; Simonyi, M. Molecular Basis of the Cotton Effects Induced by the Binding of Curcumin to Human Serum Albumin. *Tetrahedron: Asymmetry* **2003**, *14*, 2433−2444.
(29) Hoffmann, R. W. Flexible Molecules with Defined Shape-Conformational Design. *Angew. Chem., Int. Ed.* **1992**, *31*, 1124−1134.

(30) Chaudret, R.; de Courcy, B.; Contreras-García, J.; Gloaguen, E.; Zehnacker-Rentien, A.; Mons, M.; Piquemal, J.-P. Unraveling on-covalent Interactions within Flexible Biomolecules: from Electron Density Topology to Gas Phase Spectroscopy. *Phys. Chem. Chem. Phys.* **2014**, *16*, 9876−9891.
(31) IUPAC. Compendium of Chemical Terminology. In (*The "Gold Book"*), 2nd ed.; Blackwell Scientific Publications: Oxford, 1997.
(32) Hohenberg, P.; Kohn, W. Inhomogeneous Electron Gas. *Phys. Rev.* **1964**, *136*, B864−B871.
(33) Kohn, W.; Sham, L. J. Self-consistent Equations Including Exchange and Correlation Effects. *Phys. Rev. A* **1965**, *140*, A1133−A1138.
(34) Frisch, M. J.; Trucks, G. W.; Schlegel, H. B.et al. *Gaussian 16*, Revision C.01; Gaussian, Inc., 2016.
(35) Rusydi, F.; Madinah, R.; Puspitasari, I.; Mark-Lee, W. F.; Ahmad, A.; Rusydi, A. Teaching Reaction Kinetics Through Isomerization Cases with the Basis of Density-functional Calculations. *Biochem. Mol. Biol. Educ.* **2021**, *49*, 216−227.
(36) Becke, A. D. Densityfunctional Thermochemistry. III. The Role of Exact Exchange. *J. Chem. Phys.* **1993**, *98*, 5648−5652.
(37) Grimme, S.; Antony, J.; Ehrlich, S.; Krieg, H. A consistent and accurate ab initio parametrization of density functional dispersion correction (DFT-D) for the 94 elements H-Pu. *J. Chem. Phys.* **2010**, *132*, No. 154104, DOI: 10.1063/1.3382344.
(38) Austin, A.; Petersson, G. A.; Frisch, M. J.; Dobek, F. J.; Scalmani, G.; Throssell, K. A Density Functional with Spherical Atom Dispersion Terms. *J. Chem. Theory Comput.* **2012**, *8*, 4989−5007.
(39) Zhao, Y.; Truhlar, D. G. The M06 Suite of Density Functionals for Main Group Thermochemistry, Thermochemical Kinetics, Noncovalent Interactions, Excited States, and Transition Elements: Two New Functionals and Systematic Testing of Four M06-class Functionals and 12 Other Functionals. *Theor. Chem. Acc.* **2008**, *120*, 215−241.
(40) Yanai, T.; Tew, D. P.; Handy, N. C. A New Hybrid Exchangecorrelation Functional Using the Coulomb-attenuating Method (CAM-B3LYP). *Chem. Phys. Lett.* **2004**, *393*, 51−57.
(41) Ilawe, N. V.; Zimmerman, J. A.; Wong, B. M. Breaking Badly: DFT-D2 Gives Sizeable Errors for Tensile Strengths in Palladium-Hydride Solids. *J. Chem. Theory Comput.* **2015**, *11*, 5426−5435.
(42) Lee, J.-H.; Park, J.-H.; Soon, A. Assessing the influence of van der Waals corrected exchange-correlation functionals on the anisotropic mechanical properties of coinage metals. *Phys. Rev. B* **2016**, *94*, 024108−1−024108−11.
(43) Hermann, J., Jr.; DiStasio, R. A.; Tkatchenko, A. First-Principles Models for van der Waals Interactions in Molecules and Materials: Concepts, Theory, and Applications. *Chem. Rev.* **2017**, *117*, 4714−4758, DOI: 10.1021/acs.chemrev.6b00446.
(44) Sanphui, P.; Goud, N. R.; Khandavilli, U. B. R.; Nangia, A. Fast Dissolving Curcumin Cocrystals. *Cryst. Growth Des.* **2011**, *11*, 4135−4145.
(45) Silva, T. D.; Warner, I. M.; Fronczek, F. R. CCDC 1465072: Experimental Crystal Structure Determination, Curcumin dichloromethane solvate (CSD refcode-OJIWOV), 2016. https://www.ccdc.cam.ac.uk/structures/Search?Compound/curcumin&DatabaseToSearch/Published.
(46) Parimita, S. P.; Ramshankar, Y. V.; Suresh, S.; Row, T. N. G. Redetermination of Curcumin: (1E,4Z,6E)-5-hydroxy-1,7-bis(4-hydroxy-3-methoxyphenyl)hepta-1,4,6-trien-3-one. *Acta Crystallogr., Sect. E: Struct. Rep. Online.* **2007**, *63*, o860−o862.
(47) Reid, J. W.; Kaduk, J. A.; Garimella, S. V.; Tse, J. S. Rietveld Refinement Using Synchrotron Powder Diffraction Data for Curcumin, $C_{21}H_{20}O_6$, and Comparison with Density Functional Theory. *Powder Diffr.* **2015**, *30*, 67−75.
(48) Young, D. C. *Computational Chemistry*; John Wiley & Sons, 2001.
(49) Schreiner, P. R.; Reisenauer, H. P., IV; Pickard, F. C.; Simmonett, A. C.; Allen, W. D.; Mátyus3, E.; Császár, A. G. Capture of Hydroxymethylene and Its Fast Disappearance Through Tunnelling. *Nature* **2008**, *453*, 906−909, DOI: 10.1038/nature07010.
(50) Peters, P. S.; Duflot, D.; Faure, A.; Kahane, C.; Ceccarelli, C.; Wiesenfeld, L.; Toubine, C. Theoretical Investigation of the Isomerization of trans-HCOH to H_2CO: An Example of a Water-Catalyzed Reaction. *J. Phys. Chem. A* **2011**, *115*, 8983−8989.
(51) Schreiner, P. R.; Reisenauer, H. P.; Ley, D.; Gerbig, D.; Wu, C.-H.; Allen, W. D. Methylhydroxycarbene: Tunneling Control of a Chemical Reaction. *Science* **2011**, *332*, 1300−1303.
(52) Griffiths, D. J. *Introduction to Quantum Mechanics*, 2nd ed.; Pearson Education, 2005.
(53) Schleif, T.; Merini, M. P.; Sander, W. The Mystery of the Benzene-Oxide/Oxepin EquilibriumHeavy-Atom Tunneling Reversed by Solvent Interactions. *Angew. Chem., Int. Ed.* **2020**, *59*, 20318−20322.
(54) Schleif, T.; Merini, M. P.; Henkel, S.; Sander, W. Solvation Effects on Quantum Tunneling Reactions. *Acc. Chem. Res.* **2022**, *55*, 2180−2190.
(55) Fadilla, R. N.; Aisyah, N. D.; Dipojono, H. K.; Rusydi, F. A Theoretical Study of the Rearranging trans-HCOH to H_2CO via Quantum Tunnelling with DFT and WKB Approximation. *Procedia Eng.* **2017**, *170*, 113−118.
(56) Susanti, E. D.; Rusydi, F.; Puspitasari, I.; Fadilla, R. N.; Aisyah, N. D.; Ahmad, A. A First-principles Study on the Quantum Tunneling of Methylhydroxycarbene Isomerization in Various Solvents. *J. Phys.: Conf. Ser.* **2020**, *1568*, No. 012003, DOI: 10.1088/1742-6596/1568/1/012003.
(57) Jin, L.; Wu, Y.; Zhao, X. Theoretical Insight Into the Au(i)-catalyzed Hydration of Halo-substituted Propargyl Acetate: Dynamic Water-assisted Mechanism. *RSC Adv.* **2016**, *6*, 89836−89846.
(58) Cucinotta, C. S.; Ruini, A.; Catellani, A.; Stirling, A. Ab Initio Molecular Dynamics Study of the KetoEnol Tautomerism of Acetone in Solution. *ChemPhysChem* **2006**, *7*, 1229−1234.
(59) Rayne, S.; Forest, K. A Comparative Examination of Density Functional Performance Against the ISOL24/11 Isomerization Energy Benchmark. *Comput. Theor. Chem.* **2016**, *1090*, 147−152.

https://doi.org/10.1021/acsomega.3c04907
ACS Omega 2023, 8, 34022−34033